Published in final edited form as:
Invest Radiol. 2013 December ; 48(12): . doi:10.1097/RLI.0b013e31829a4f2f.

Quantification of Thoracic Blood Flow Using Volumetric MRI with Radial Velocity Encoding: In Vivo Validation

Alex Frydrychowicz, MD[1,2], **Oliver Wieben, PhD**[2,3,4], **Eric Niespodzany, MS**[2], **Scott B. Reeder, MD PhD**[2,3,4,5], **Kevin M. Johnson, PhD**[3], and **Christopher J. François, MD**[2]

[1]University Hospital Schleswig-Holstein, Campus Lübeck, Clinic for Radiology and Nuclear Medicine, Lübeck, Germany

[2]University of Wisconsin – Madison, Department of Radiology

[3]University of Wisconsin – Madison, Department of Medical Physics

[4]University of Wisconsin – Madison, Department of Bioengineering

[5]University of Wisconsin – Madison, Department of Medicine

Abstract

Objectives—To validate radially undersampled 5-point velocity-encoded time-resolved flow-sensitive MRI ("PC-VIPR") for quantification of ascending aortic (AAO) and main pulmonary artery (MPA) flow *in-vivo*

Materials and Methods—Data from 18 healthy volunteers (41.6±16.2years (22–73); BMI 26.0±3.5 (19.1–31.4) scanned at 3T with a 32-channel-coil were included. Left and right ventricular stroke volumes (LVSV and RVSV, respectively) calculated from contiguous short-axis CINE-bSSFP slices were used as the primary reference for cardiac output. Flow measured from 2D-PC-MRI in the AAO and MPA served as a secondary reference. Time-resolved 3-dimensional flow-sensitive MRI (4D-Flow-MRI) using PC-VIPR was performed with a velocity sensitivity V_{enc}=150cm/s reconstructed to 20 time frames at 1.4mm isotropic spatial resolution. In 11/20 subjects, phantom corrected 4D-Flow-MRI data was also assessed. Differences between methods of calculating LV and RV cardiac output were assessed with Bland-Altman analysis (BA, average difference ± 2SD). The Q_P/Q_S-ratio was calculated for each method.

Results—Initially, PCVIPR compared unfavorably to CINE-bSSFP (LVSV: 96.5±14.4ml, RVSV: 93.6±14.0mL vs. 81.2±24.3mL (AAO) and 85.6±25.4mL (MPA); p=0.027 and 0.25) with BA differences of −14.6±44.0mL (AAO) and −9.0±45.9mL (MPA). While phantom correction had minor effects on 2D-PC-MRI results and comparison to CINE-bSSFP, it improved PC-VIPR results: BA differences between CINE-bSSFP and PC-VIPR after correction were −1.4±15.3ml (AAO) and −4.1±16.1mL (MPA); BA comparison with 2D-PC-MRI improved to −12.0±48.1mL (AAO) and −2.2±19.5mL (MPA). Q_P/Q_S-ratio results for all techniques were within physiologic limits.

Corresponding author: PD Dr. med. Alex Frydrychowicz, University Hospital Schleswig-Holstein, Campus Lübeck, Clinic for Radiology and Nuclear Medicine, Ratzeburger Allee 160, 23562 Lübeck, Germany, Phone: +49-451-500-3153, Fax: +49-451-500-6493, alex.frydrychowicz@uksh.de.

Disclosures: The UW Madison receives research support from GE Healthcare. A.F. has received an education stipend from Bracco Diagnostics.

Conclusions—Accurate quantification of AAO and MPA flows with radially undersampled 4D-Flow-MRI applying 5-point velocity encoding is achievable when phantom correction is used.

Keywords

flow quantification; phase contrast MRI; 4D flow MRI; magnetic resonance imaging

INTRODUCTION

Four-dimensional, flow-sensitive magnetic resonance imaging (4D-Flow-MRI) acquisitions, which acquire time-resolved, three-dimensional, three-directionally velocity-encoded data, have become increasingly used for cardiovascular imaging. 4D-Flow-MRI has the advantage of simultaneous acquisition of both morphological and hemodynamic data. The flow information can be evaluated both qualitatively and quantitatively, including streamline and particles trace visualization, calculation of flow volumes, pulse wave velocity estimation, derivation of wall shear stress, and other hemodynamic parameters [1, 2]. Earlier efforts to establish this technique have shown physiological and non-physiological blood flow patterns [3, 4]. There is an increasing number of clinical studies using 4D-Flow-MRI for the analysis of form-function-interdependencies in normal volunteers [3, 5, 6] and patients, such as those with bicuspid aortic valves [7], ascending aortic aneurysms [8] and aortic coarctation [9, 10] as well as intracardiac flows [11, 12] among others. Extra-thoracic vascular territories have also been evaluated, including craniocervical [13–15] as well as mesenteric and splanchnic vasculature [16, 17].

Most 4D-Flow-MRI methods are based on Cartesian acquisitions with scan protocols that limit the imaging volume to maintain clinically feasible scan times, thereby requiring careful planning to tailor the imaging slab to the anatomy of interest. Alternatively, 4D-Flow-MRI can be performed with undersampled, e.g., inherently accelerated, acquisition schemes, such as PC-VIPR (Phase Contrast Vastly undersampled imaging with Isotropic resolution Projection Reconstruction MR [18]). With PC-VIPR, larger regions such as the entire head or thorax can be acquired in a single scan in significantly reduced scan times by applying the principles of radial undersampling. Large volume acquisitions with high spatial resolution imaging with improved signal to noise ratio (SNR) can be achieved in clinical feasible scan times through the use of 5-point velocity encoding methods [19, 20].

However, there are many potential sources of error in flow quantification, including gradient non-linearity and eddy currents [21]. Therefore, it is important to validate any new flow quantification method using established standard sequences. The primary aim of this study was to conduct an *in-vivo* validation for 5-point PC-VIPR for the assessment of flow in the ascending aortic (AAO) and main pulmonary arterial (MPA). Using CINE balanced steady state free precession (bSSFP) cardiac volumetry as the clinically accepted reference standards, we compared flow measured in the ascending aorta and the main pulmonary artery (MPA) using PC-VIPR to left and right ventricular stroke volumes (LVSV and RVSV, respectively). Secondary aims of this study included (a) comparison of flow measured in the AAO and MPA using PC-VIPR to a clinical standard product, a prospectively ECG-triggered 2-dimensional phase contrast MRI with 1-directional velocity encoding (2D-PC-MRI) and b) calculation and comparison of Q_P/Q_S ratios using all approaches.

METHODS AND MATERIALS

Study participants

This Health Insurance Portability and Accountability Act (HIPAA-) compliant study was conducted after approval of the local Institutional Review Board and written informed consent was obtained from all subjects. Participants were recruited from a database of healthy volunteers. Exclusion criteria included standard contraindications to MRI (e.g., metallic devices, claustrophobia), contraindications to gadolinium based contrast agents, high cardiovascular risk factors (body mass index BMI > 30, a history of smoking, diabetes, or hypertension), and drugs affecting the cardiovascular function (e.g., beta-blockers). In total, twenty volunteers were included. During the examinations and after analysis of recorded ECG-data during the scan, two volunteers were excluded from the final analysis due to severe arrhythmia (n=1) and poor (i.e., irregular, although no apparent arrhythmia was known) ECG-trigger-quality (n=1). In total, data from 18 volunteers (41.6 ± 16.21 years [22.5–73.5]; BMI 26.0 ± 3.5 [19.1–31.4]; nine women, nine men; nine under the age of 35, nine above) were included in the analysis.

MR Imaging

MR acquisitions were performed on a 3T clinical scanner (Discovery MR 750, GE Healthcare, Waukesha, WI) using a 32-channel phased-array abdominal coil (NeoCoil, Pewaukee, WI). Participants were scanned head first in the supine position. After completion of the study, flow sequences (2D and 4D) were repeated on a large static phantom in 11 cases using the same settings used for the individual volunteer acquisitions.

CINE-bSSFP volumetry—To obtain end-diastolic and end-systolic right and left ventricular volumes a retrospectively ECG-triggered CINE balanced steady state free precession (bSSFP) sequence was performed per clinical standard during multiple breathholds. Both ventricles were imaged with contiguous short axis slices positioned orthogonal to the interventricular septum. Typical imaging parameters included: repetition time/echo time (TR/TE) = 3.12/1.14ms; flip angle (FA) = 45°; FOV = 390mm × 390mm, acquisition matrix 224 × 140 with fractional echo readout, slice thickness (SLT) = 8mm, interpolated to a spatial resolution of = 1.5 × 1.5 ×8mm^3. Depending upon the heart rate, a k-space segmentation factor of 12–16 views per segment was used for a temporal resolution of approximately 36–48 ms. Images were interpolated to 25 cardiac frames through the cardiac cycle.

4D phase contrast with PC-VIPR—An investigational sequence applying a 5-point velocity-encoded, time-resolved 3-dimensional phase contrast sequence was used („5-point PC-VIPR“). Radial undersampling (Phase Contrast Vastly undersampled Isotropic-voxel radial Projection Reconstruction imaging, ‘PC-VIPR’) was applied for time-efficient large volume coverage with high spatial and temporal resolution. 5-point velocity encoding was chosen due to its increased velocity encoding sensitivity range at the expense of a small scan time-penalty [20]. Imaging parameters for PC-VIPR included: dual echo acquisition for improved sampling efficiency, (TR/TE) = 6.1–7.8/2.1–3.2ms (first echo), imaging volume = 32cm (R/L) × 32cm (A/P) × 22 (S/I) cm, acquired isotropic spatial resolution of 1.4 mm, receiver bandwidth = +−125 kHz, axial slab excitation, typical FA = 14°, and velocity encoding sensitivity V_{enc}=150cm/s. An adaptive respiratory gating scheme using respiratory bellows and a 55% acceptance rate resulted in scan times of approximately 10–12min depending on the respiratory rate and pattern of the subject. During the approximately 5 min of actual acquisition time in the expiration plateau of the respiration cycle, a total of 110,000 echoes were recorded from 55,000 excitations at 22,000 unique projection angles. This corresponds to an undersampling factor of 3.6 for a single, time averaged acquisition

volume. However, the individual cardiac frames are much higher undersampled as retrospective ECG-gating was used to reconstruct 20 time frames through the cardiac cycle. This was achieved with temporal filtering similar to view sharing in Cartesian acquisitions [22], which makes the undersampling factor dependent on the k-space position, here corresponding to 4xTR in the center of k-space and 40xTR on the outer edge of k-space.

Automatic correction for Maxwell terms [23] and eddy currents using 2^{nd} order polynomials [24] was included in the image acquisition and post-processing scheme (software corrected data). After an interim analysis of data indicating large discrepancies between PCVIPR and bSSFP, a second post-processing routine in the subset of eleven volunteers was applied in which the automatic correction was switched off. Instead, static phantom data were reconstructed using the same spatiotemporal settings. Results from both volunteer and phantom data set were subtracted following the procedure described by Chernobelsky et al. [25] (phantom corrected data, see Figure 1).

2D-PC-MRI—2D phase contrast imaging was performed in a supra-coronary ascending aortic plane (AAO) and a supra-valvular plane placed in the main pulmonary artery (MPA) with a prospectively ECG-triggered spoiled gradient echo sequence. Specific imaging settings were adapted to optimize temporal resolution within breath hold limitations (≤24sec). Typical imaging parameters were dependent on the heart rate and included: velocity encoding sensitivity V_{enc}=150cm/s, TR/TE = 5.15/2.94ms; FA = 30°; slice thickness (SLT) = 7mm; FOV = 370×370mm; acquisition matrix = 256 × 128 interpolated to a spatial resolution of 1.45 × 1.45 × 7mm^3. Depending upon the heart rate, a segmentation factor of 4–8 was used. These settings resulted in 19.7 ± 4.7 (13–37) recorded time frames.

Contrast-Enhanced MR-angiography (CE-MRA)—To assist planning of 2D-PC-MRI slice prescription and improve vascular signal on the subsequent 2D-PC-MRI and PC-VIPR acquisitions [26], contrast-enhanced MR-angiography was performed using 0.03mmol/kg gadofosveset trisodium (Ablavar®, Lantheus, Billerica, MA) injected at 0.6ml/s followed by a 30ml saline chaser injected the same rate, using a power injector. The CE-MRA protocol consisted of a 3D spoiled gradient echo sequence applying parallel imaging based on a data-driven approach [ARC (autocalibrated reconstruction), net acceleration factor = 3.56 [27]]. Specific imaging details were adapted to each individual's anatomy with a typical spatial resolution of 0.9 × 1.4 × 2.0 mm reconstructed to a resolution of 0.5 × 0.7 × 1.0 mm through zero-filling.

Data analysis

CINE-bSSFP analysis of LVSV and RVSV—Analysis of the CINE-bSSFP images was performed by an experienced radiologist blinded to the results of the other sequences on an Advantage Windows workstation using ReportCard 2.0 (GE Healthcare, Waukesha, WI). Both right ventricular (RV) and left ventricular (LV) endocardial contours were delineated on end-diastolic and end-systolic frames visually determined by maximum and minimum ventricle volumes, respectively. RV and LV volumes were quantified using Simpson's rule by adding volumes of individual slices. RV and LV stroke volumes (SV) were quantified by subtraction of end-systolic volume (ESV) from end-diastolic volume (EDV).

AAO and MPA flow analysis on 2D-PC-MRI data—Analysis of 2D-PC-MRI data was performed blinded to the CINE-bSSFP and 4D PC-VIPR results on an Advantage Windows workstation (GE Healthcare, Waukesha, WI). For each acquired frame, the luminal contour was manually drawn (or, in case of automatic propagation, manually confirmed or corrected). Contours were saved and copied directly to the phantom data to guarantee perfect co-registration for a subsequent phase correction. To compensate for the time lag

between R-wave trigger and start of data acquisition, missing 2D-PC-MRI flow data was extrapolated using the late diastolic baseline and the first acquired time point on the flow curve. In detail, the mean diastolic flow per time frame was determined by averaging the last 5 diastolic time frames. Then, the scan duration was subtracted from the RR-duration (both provided by the scanner). The remainder was divided by the temporal resolution and multiplied by the determined diastolic flow per frame.

AAO and MPA flow analysis on PC-VIPR data—A flowchart detailing the post-processing steps for software and phantom based post-processing is given in Fig. 1. After completion of each scan, the acquired k-space PC-VIPR data were transferred for offline reconstruction and data post-processing. Using a Matlab-based software script (The Mathworks, Natick, MA), both software and phantom corrected data were converted for use in EnSight, a commercially available software tool used for 3D morphologic and hemodynamic visualization (v9.1, CEI, Apex, NC).

In EnSight, software corrected data were visualized using a 3D shaded surface display to guide the placement of square 2D cut-planes in the supra-coronary ascending aorta and the main pulmonary artery (Figure 2). The cut-plane orientation and geometry within the dataset was saved and data were exported to a Matlab-based quantification script extensively used in other groups [28]. Subsequently, the saved cut-plane details were applied to the phantom corrected data to guarantee exact data comparability. Segmentation of data was performed manually in a similar fashion. Luminal contours of both AAO and MPA were segmented on basis of the software-corrected data. Segmentation outlines were saved and applied to the phantom corrected data.

Q_P/Q_S ratio—In all LVSV and RVSV or AAO and MPA data pairs the Q_P/Q_S-ratio was determined from the quotient of pulmonary arterial flow and ascending aortic flow.

Statistical analysis

Descriptive statistics are presented as average ± standard deviation. Results between age groups were compared using a two-sided, unpaired Student's t-test accepting a $p<0.05$ as indicative of statistical significance. For statistical comparison of AAO and MPA flows (LV SV and RV SV, respectively) as well as calculated Q_P/Q_S ratio, a paired two-sided t-test was used. Bland-Altman analysis was performed because there was no true reference ('gold') standard. Two standard deviations (± 10%) were used following [29]. Data from Bland-Altman comparisons are summarized as bias (mean difference between results of both techniques) ± 2SD. Accepting CINE-bSSFP volumetry as the *de facto* clinical standard, linear regression was added and correction coefficients (r^2) are given for correlation.

RESULTS

Detailed results are summarized in Table 1 and Figure 3. For non-phantom-corrected data, there was good agreement between (a) CINE-bSSFP measurement of LVSV and RVSV (96.5±14.4ml and 93.6±14.0mL) and (b) 2D-PC-MRI measurement of AAO and MPA flow (98.0±21.8mL and 90.0±18.8mL), respectively. Differences varied insignificantly. Greater differences were observed between CINE-bSSFP and PC-VIPR (AAO = 81.2±24.3mL; MPA = 85.6±25.4mL). The comparison revealed a statistically significant underestimation of flow by PC-VIPR; Bland Altman comparison −14.6 ± 44.0mL and −9.0 ± 45.9mL, respectively with weak correlation coefficients of $r^2 = 0.23$ and 0.21, respectively. The statistical comparison of PC-VIPR and 2D-PC-MRI data differences was also statistically different and resulted in a weak to moderate correlation of $r^2 = 0.51$ (AAO) and 0.25 (MPA). Phantom correction of data markedly improved the agreement between 5-point PC-

VIPR (AAO = 95.9 ± 19.1mL; MPA = 90.3 ± 13.7mL) and CINE-bSSFP (BA −1.4 ± 15.3 and −4.1 ± 16.1; correlation R^2 0.86 and 0.71). The comparison between 2D-PC-MRI and 5-point PC-VIPR was improved with respect to AAO results while MPA correlation was strong already (see Table 1). It has to be noted, that pooling of both MPA and AAO results provided improved results for correlation for all comparisons (see Figure 2).

For clinical applicability, the Q_P/Q_S ratio was determined for each technique on basis of the phantom corrected data. The graphic representation of results is displayed in Figure 4. The observed ratios from all imaging techniques were in the expected physiological range: CINE-bSSFP = 0.97 ± 0.04, 2D-PC-MRI = 0.96 ± 0.09. PC-VIPR = 0.95 ± 0.06 with a Bland Altman bias of 0.02 ± 0.07 between CINE-bSSFP and PC-VIPR underlining a slight underestimation by PC-VIPR relative to CINE-bSSFP. No statistical significance was revealed between results. Greater variability in 5-point PC-VIPR data was observed.

DISCUSSION

Four-dimensional MR imaging of blood flow in various body regions and based on solutions by various vendors holds promise for a comprehensive hemodynamic assessment. However, relatively few in-vivo validation studies have been performed to validate these methods [30], due in part to the lack of a reliable reference standard. Furthermore, phase related errors can be platform and vendor dependent, partially attributed to uncompensated eddy currents in fast imaging systems and varying post-processing correction techniques [21]. Therefore, results with specific sequences on scanners of a specific vendor may not be transferred to another, de novo testing of an introduced sequence is required. While in-vitro studies using idealized conditions and flow phantoms are necessary as a proof of concept, they are of limited use in human subjects due to the potential errors introduced when scanning in a clinical environment. Hence, in-vivo studies testing the sequence in comparison to the available standards of reference are necessary. In this study we used RV and LV stroke volumes using CINE-bSSFP as primary and MPA and AAO flow using 2D-PC-MRI as secondary clinical reference standards [31].

The results of our study suggest accurate flow quantification in the AAO and MPA is possible with PC-VIPR; however, additional data from a phantom scan are required for background phase offset corrections. Large offsets between software-corrected and reference standards suggest that the currently implemented automated software correction for eddy currents is inferior to the phantom correction. Phantom corrections in 2D PC also improved correlation with CINE-bSSFP, but changes were smaller as compared to PC-VIPR/CINE-bSSFP and differences were not significant. Given this, in its current implementation, PC-VIPR is either more sensitive to background phase offsets or the automatic phase correction algorithm was inaccurate. Therefore, we believe that absolute quantification with the technique should, at its present stage of implementation, not be performed without phantom correction. This includes increased scan times.

Alternatively, the standard derating of gradient performance in clinical 2D-PC-MRI (‘flow optimization’ flag set to ‘on’) may have decreased inaccuracies as opposed to maximum gradient performance during PC-VIPR 4D-Flow-MR.

This is somewhat contradictory to a recently published work on multi-point encoding on a scanner of a different vendor [32]. It therefore seems less likely that the errors are sequence-based and more likely that errors are either based on a suboptimal automatic correction and/or gradient power. Finally, inaccuracies due to “misplacement” of the imaging volume are possible. Although special care was taken to place the center of the imaging plane in a

correct position centered over the aorta minor differences due to patient motion or with respect to MPA flows might be explained.

In this study, we focused only on AAO and MPA flow quantification. However, PC-VIPR data allows for derivation of a wide variety of flow-related parameters that might be used as biomarkers of vascular health or disease status [2]. This capability of radially undersampled PC-VIPR to reliably sample such data will also need to be demonstrated in other regions of the body. The practical advantages of using a radially undersampled approach are the imaging speed and the large volume of coverage of the sequence. Both make it an attractive approach to imaging larger cardiovascular territories for applications such as congenital heart disease [33] and the hepatic vasculature [16].

It should be noted that in both congenital heart disease and imaging of the hepatic vasculature, slow flow conditions are often encountered. The study presented here focuses primarily on high flow conditions in the thoracic aorta and main pulmonary arteries. To achieve similar agreement between methods in low flow conditions, the velocity encoding sensitivity must to be adjusted appropriately. By doing so, aliasing occurs in high flow vessels can occur and is often a challenging problem. Alternatively, dual V_{enc} approaches that acquire two scans, one with a low and one with a higher velocity encoding sensitivity can be performed, improving the range of velocity sensitivities, but at the cost of doubled scan time. The challenge of velocity encoding is not specific to radially undersampled scans and also impacts Cartesian acquisition strategies. Recent results have presented other alternatives that combine the scan time gain in radial undersampling with partial acquisition of different velocity encoding sensitivities [34]. In addition, the analysis is based on data using a strong albumin-bound Gadolinium-based contrast agent. Bock et al. have shown superiority in image quality of so-called “blood-pool” agents as opposed to non-enhanced scans or scans with lower albumin binding capacity [26]. Thus, results should not be uncritically transferred to unenhanced scans which may exhibit different validity due to systems. Therefore, a transfer to 1.5T would likely result in a decreased SNR or, to keep the SNR at a comparable level, in e.g. resulting in longer acquisition times or using increased voxels sizes. However, the use of a Gadolinium-based contrast agent may impose potential risks to participants or patients. Hence, standard clinical procedures to limit the risk of contrast material-induced potential side effects should be applied.

Another drawback may be seen in the use of a prospectively ECG-gated 2D sequence, encountering a time-lag between ECG-signal and start of the scan, and the related need for data interpolation. Without question, a retrospectively gated scan would have been optimal. However, PC-VIPR was tested against the clinical routine settings on our scanners that provide a previously validated, prospectively 2D PC sequence [35]. Phantom correction provides certainty with respect to unwanted phase offset contribution [21]. Although a three-directionally velocity encoded sequence is available, the vendor does not offer a 3D PC product sequence.

Lastly, it has to be noted, that the relatively long acquisition times may lead to an effective averaging of flow parameters or features. Also, small variations between results may have been introduced by data acquisition during free breathing (4D PC MRI) as opposed to inspiratory breath holding (CINE-bSSFP and 2D PC MRI) that are expected to play a minor role in arterial hemodynamics as opposed to venous thoracic flow.

In conclusion, our data demonstrate that radially undersampled flow-sensitive phase contrast MRI using PC-VIPR can be used in clinical routine. Further, phantom correction should be used with 4D flow MRI for the most accurate quantification of blood flow.

Acknowledgments

The authors would like to express their gratitude for the continuous support of the MR technicians Kelli Hellenbrand and Sara Pladziewicz. Also, Karl Vigen, PhD, has greatly contributed through technical support. Aurélien Stalder, PhD, has kindly provided the MatLab based quantification software. Further, the authors would like to acknowledge grant support from the National Institute of Health (NIH), Bracco Diagnostics, and the Research and Development committee of the Department of Radiology, University of Wisconsin – Madison.

Grant support: The authors acknowledge NIH grant support partially contributing to this project R01HL72260 (OW)

References

1. Markl M, Kilner PJ, Ebbers T. Comprehensive 4D velocity mapping of the heart and great vessels by cardiovascular magnetic resonance. Journal of cardiovascular magnetic resonance : official journal of the Society for Cardiovascular Magnetic Resonance. 2011; 13:7. [PubMed: 21235751]
2. Frydrychowicz A, Francois CJ, Turski PA. Four-dimensional phase contrast magnetic resonance angiography: potential clinical applications. European journal of radiology. 2011; 80:24–35. [PubMed: 21333479]
3. Bogren HG, Buonocore MH. 4D magnetic resonance velocity mapping of blood flow patterns in the aorta in young vs. elderly normal subjects. J Magn Reson Imaging. 1999; 10:861–869. [PubMed: 10548800]
4. Bogren HG, Buonocore MH, Valente RJ. Four-dimensional magnetic resonance velocity mapping of blood flow patterns in the aorta in patients with atherosclerotic coronary artery disease compared to age-matched normal subjects. J Magn Reson Imaging. 2004; 19:417–427. [PubMed: 15065165]
5. Frydrychowicz A, Berger A, Munoz Del Rio A, et al. Interdependencies of aortic arch secondary flow patterns, geometry, and age analysed by 4-dimensional phase contrast magnetic resonance imaging at 3 Tesla. European radiology. 2012; 22:1122–1130. [PubMed: 22207269]
6. Kilner PJ, Yang GZ, Mohiaddin RH, et al. Helical and retrograde secondary flow patterns in the aortic arch studied by three-directional magnetic resonance velocity mapping. Circulation. 1993; 88:2235–2247. [PubMed: 8222118]
7. Hope MD, Hope TA, Meadows AK, et al. Bicuspid aortic valve: four-dimensional MR evaluation of ascending aortic systolic flow patterns. Radiology. 2010; 255:53–61. [PubMed: 20308444]
8. Hope TA, Markl M, Wigstrom L, et al. Comparison of flow patterns in ascending aortic aneurysms and volunteers using four-dimensional magnetic resonance velocity mapping. J Magn Reson Imaging. 2007; 26:1471–1479. [PubMed: 17968892]
9. Frydrychowicz A, Markl M, Hirtler D, et al. Aortic hemodynamics in patients with and without repair of aortic coarctation: in vivo analysis by 4D flow-sensitive magnetic resonance imaging. Invest Radiol. 2011; 46:317–325. [PubMed: 21285892]
10. Hope MD, Meadows AK, Hope TA, et al. Clinical evaluation of aortic coarctation with 4D flow MR imaging. J Magn Reson Imaging. 2010; 31:711–718. [PubMed: 20187217]
11. Bolger AF, Heiberg E, Karlsson M, et al. Transit of blood flow through the human left ventricle mapped by cardiovascular magnetic resonance. J Cardiovasc Magn Reson. 2007; 9:741–747. [PubMed: 17891610]
12. Dyverfeldt P, Kvitting JP, Sigfridsson A, et al. Assessment of fluctuating velocities in disturbed cardiovascular blood flow: in vivo feasibility of generalized phase-contrast MRI. J Magn Reson Imaging. 2008; 28:655–663. [PubMed: 18777557]
13. Wetzel S, Meckel S, Frydrychowicz A, et al. In vivo assessment and visualization of intracranial arterial hemodynamics with flow-sensitized 4D MR imaging at 3T. AJNR Am J Neuroradiol. 2007; 28:433–438. [PubMed: 17353308]
14. Harloff A, Albrecht F, Spreer J, et al. 3D blood flow characteristics in the carotid artery bifurcation assessed by flow-sensitive 4D MRI at 3T. Magnetic resonance in medicine : official journal of the Society of Magnetic Resonance in Medicine / Society of Magnetic Resonance in Medicine. 2009; 61:65–74. [PubMed: 19097219]

15. Markl M, Wegent F, Zech T, et al. In vivo wall shear stress distribution in the carotid artery: effect of bifurcation geometry, internal carotid artery stenosis, and recanalization therapy. Circulation Cardiovascular imaging. 2010; 3:647–655. [PubMed: 20847189]
16. Frydrychowicz A, Landgraf BR, Niespodzany E, et al. Four-dimensional velocity mapping of the hepatic and splanchnic vasculature with radial sampling at 3 tesla: A feasibility study in portal hypertension. Journal of magnetic resonance imaging : JMRI. 2011; 34:577–584. [PubMed: 21751287]
17. Stankovic Z, Frydrychowicz A, Csatari Z, et al. MR-based visualization and quantification of three-dimensional flow characteristics in the portal venous system. J Magn Reson Imaging. 2010; 32:466–475. [PubMed: 20677279]
18. Gu T, Korosec FR, Block WF, et al. PC VIPR: a high-speed 3D phase-contrast method for flow quantification and high-resolution angiography. AJNR Am J Neuroradiol. 2005; 26:743–749. [PubMed: 15814915]
19. Pelc NJ, Bernstein MA, Shimakawa A, et al. Encoding strategies for three-direction phase-contrast MR imaging of flow. J Magn Reson Imaging. 1991; 1:405–413. [PubMed: 1790362]
20. Johnson KM, Markl M. Improved SNR in phase contrast velocimetry with five-point balanced flow encoding. Magn Reson Med. 2010; 63:349–355. [PubMed: 20099326]
21. Gatehouse PD, Rolf MP, Graves MJ, et al. Flow measurement by cardiovascular magnetic resonance: a multi-centre multi-vendor study of background phase offset errors that can compromise the accuracy of derived regurgitant or shunt flow measurements. J Cardiovasc Magn Reson. 2010; 12:5. [PubMed: 20074359]
22. Liu J, Redmond MJ, Brodsky EK, et al. Generation and visualization of four-dimensional MR angiography data using an undersampled 3-D projection trajectory. IEEE Trans Med Imaging. 2006; 25:148–157. [PubMed: 16468449]
23. Bernstein MA, Zhou XJ, Polzin JA, et al. Concomitant gradient terms in phase contrast MR: analysis and correction. Magn Reson Med. 1998; 39:300–308. [PubMed: 9469714]
24. Walker PG, Cranney GB, Scheidegger MB, et al. Semiautomated method for noise reduction and background phase error correction in MR phase velocity data. J Magn Reson Imaging. 1993; 3:521–530. [PubMed: 8324312]
25. Chernobelsky A, Shubayev O, Comeau CR, et al. Baseline correction of phase contrast images improves quantification of blood flow in the great vessels. J Cardiovasc Magn Reson. 2007; 9:681–685. [PubMed: 17578724]
26. Bock J, Frydrychowicz A, Stalder AF, et al. 4D phase contrast MRI at 3 T: effect of standard and blood-pool contrast agents on SNR, PC-MRA, and blood flow visualization. Magn Reson Med. 2010; 63:330–338. [PubMed: 20024953]
27. Brau AC, Beatty PJ, Skare S, et al. Comparison of reconstruction accuracy and efficiency among autocalibrating data-driven parallel imaging methods. Magn Reson Med. 2008; 59:382–395. [PubMed: 18228603]
28. Stalder AF, Russe MF, Frydrychowicz A, et al. Quantitative 2D and 3D phase contrast MRI: optimized analysis of blood flow and vessel wall parameters. Magn Reson Med. 2008; 60:1218–1231. [PubMed: 18956416]
29. Bland JM, Altman DG. Statistical methods for assessing agreement between two methods of clinical measurement. Lancet. 1986; 1:307–310. [PubMed: 2868172]
30. Nordmeyer S, Riesenkampff E, Crelier G, et al. Flow-sensitive four-dimensional cine magnetic resonance imaging for offline blood flow quantification in multiple vessels: a validation study. J Magn Reson Imaging. 2010; 32:677–683. [PubMed: 20815066]
31. Devos DG, Kilner PJ. Calculations of cardiovascular shunts and regurgitation using magnetic resonance ventricular volume and aortic and pulmonary flow measurements. Eur Radiol. 2009
32. Espe EK, Aronsen JM, Skrbic B, et al. Improved MR phase-contrast velocimetry using a novel nine-point balanced motion-encoding scheme with increased robustness to eddy current effects. Magnetic resonance in medicine : official journal of the Society of Magnetic Resonance in Medicine / Society of Magnetic Resonance in Medicine. 2013; 69:48–61. [PubMed: 22392844]
33. Francois CJ, Srinivasan S, Schiebler ML, et al. 4D cardiovascular magnetic resonance velocity mapping of alterations of right heart flow patterns and main pulmonary artery hemodynamics in

tetralogy of Fallot. Journal of cardiovascular magnetic resonance : official journal of the Society for Cardiovascular Magnetic Resonance. 2012; 14:16. [PubMed: 22313680]

34. Nett EJ, Johnson KM, Frydrychowicz A, et al. Four-dimensional phase contrast MRI with accelerated dual velocity encoding. Journal of magnetic resonance imaging : JMRI. 2012; 35:1462–1471. [PubMed: 22282344]
35. Wentland AL, Grist TM, Wieben O. Repeatability and Internal Consistency of Abdominal 2D and 4D Phase Contrast MR Flow Measurements. Academic Radiology. 2013

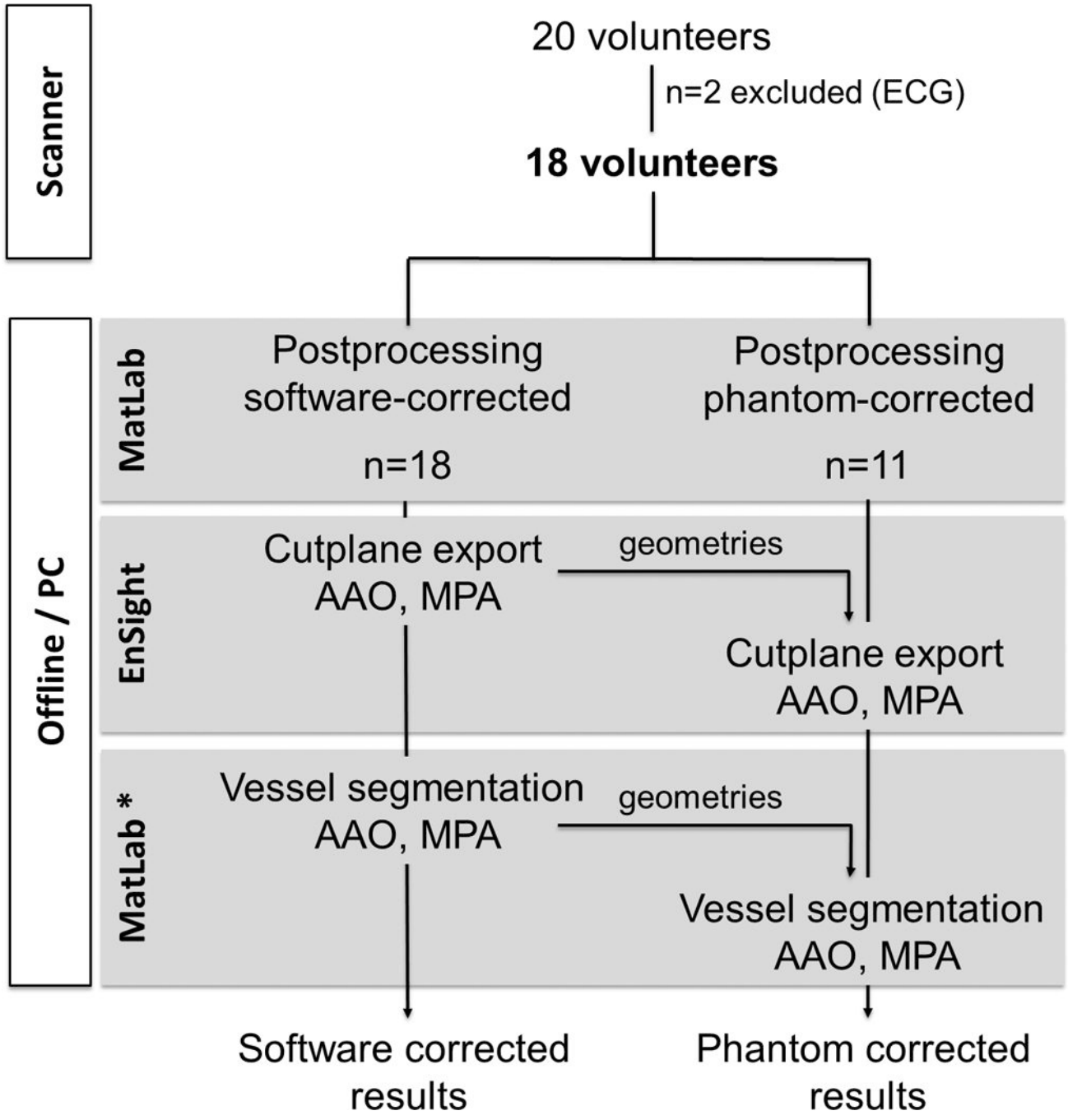

Fig. 1.
Flow chart on data handling and processing. For details please refer to Methods and Materials section. Asterisk (*) indicates work by Stalder et al. [28]

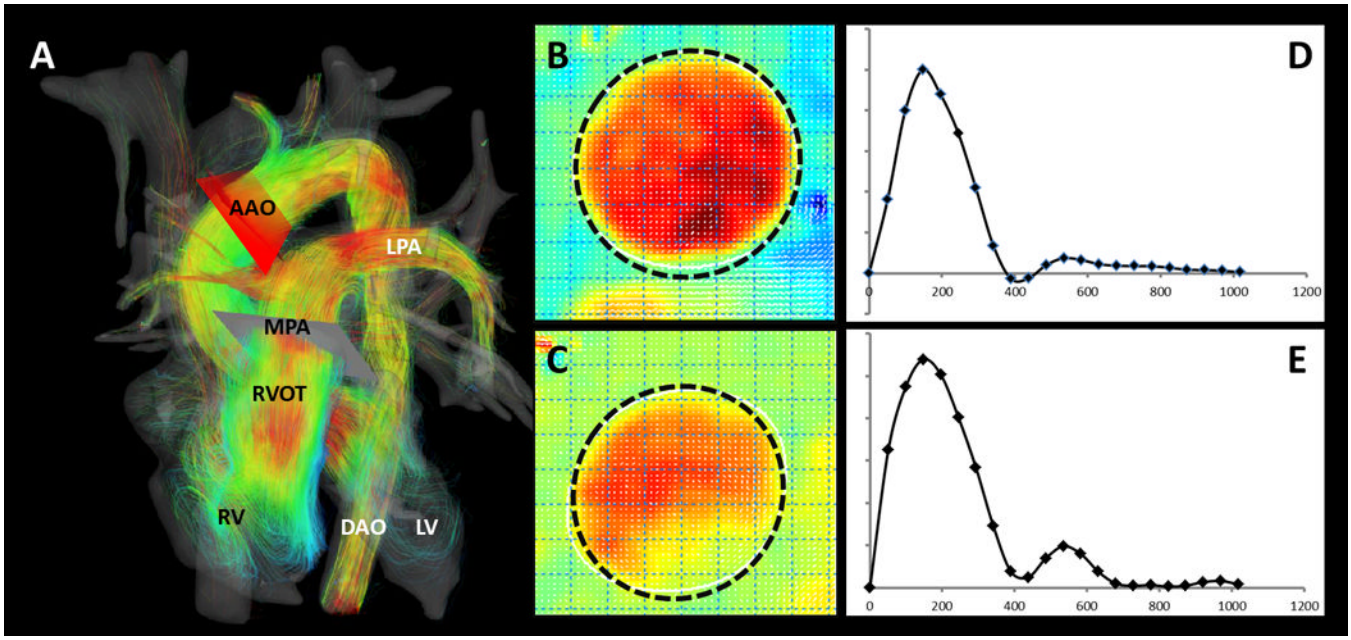

Fig. 2.

Visualization of data (A) and export of cutplanes for AAO (B) and MPA (C) flow quantification (D, E). Data was subsequently segmented and quantified in a MatLab-based software tool [28]. AAO = ascending aorta; MPA = main pulmonary artery; RVOT = right outflow tract, respectively; LPA = left pulmonary artery; DAO = descending aorta; RV and LV = right and left ventricle, respectively.

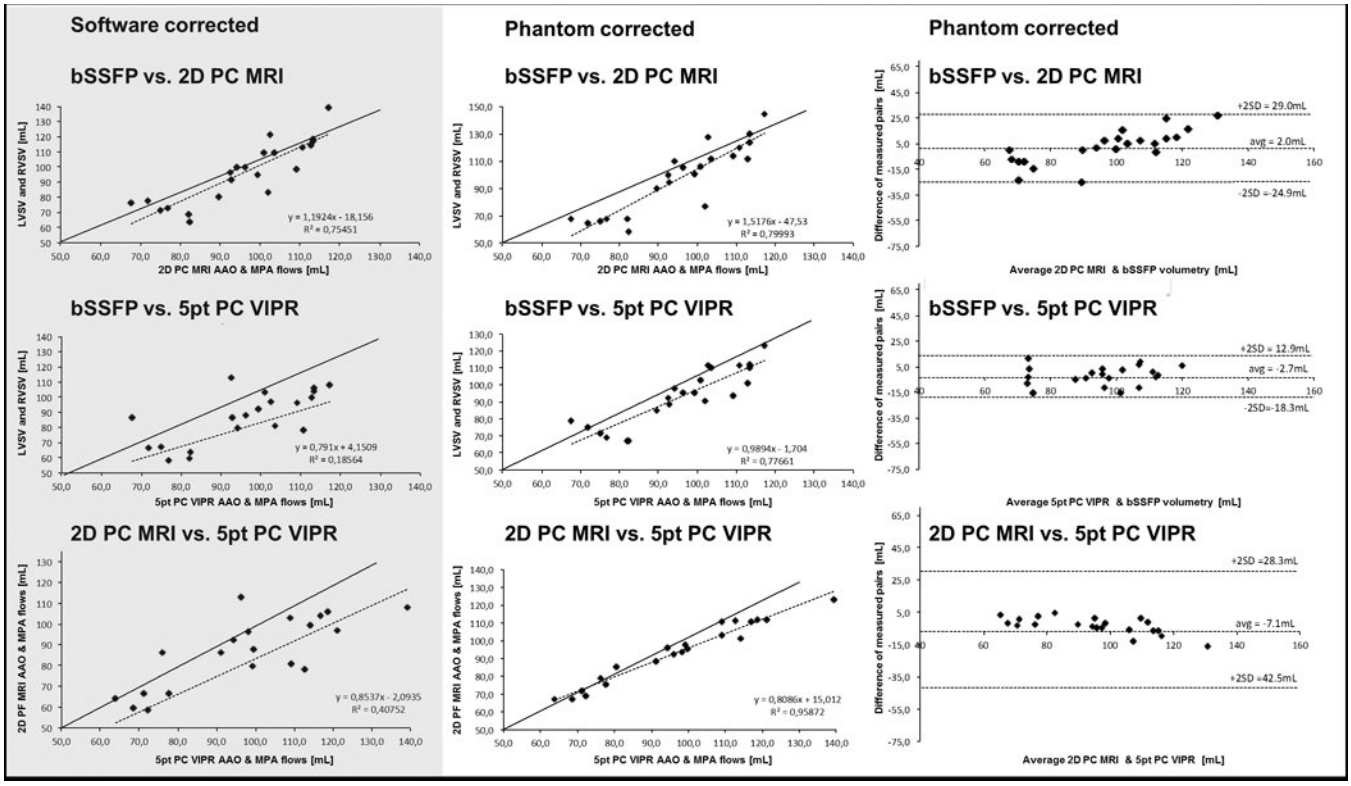

Fig. 3.

Data overview of both aortic and pulmonary arterial flows as quantified by CINE-bSSFP cardiac volumetry, 2D-PC-MRI, and 5-point PC-VIPR using PC-VIPR (5pt PC-VIPR) in n=11 volunteers based on software correction (grey shaded) and phantom corrected data. Results on all 18 volunteers with software corrected data or detailed AAO and MPA values can be found in Table 1. In the scatter plots, the solid line indicates equality of results; the dashed line indicates the trendline. In the Bland Altman plots, dashed lines are set at the average difference between individual measurement pairs (bias) and at 2 standard deviations (2SD). Of note, correlation is given as a summary of pooled MPA and AAO data.

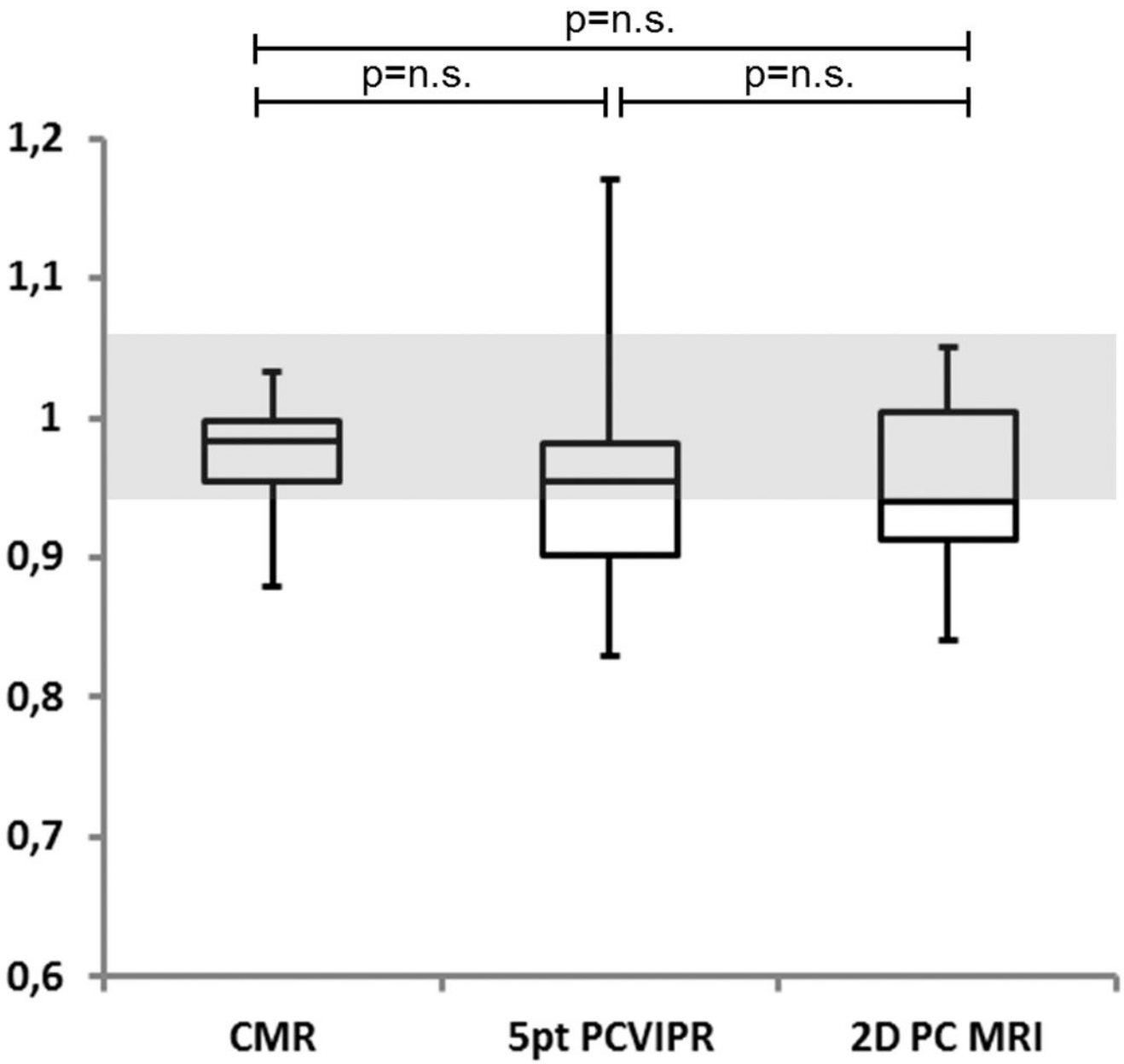

Fig. 4.

Box plot of Q_P/Q_S ratio determination based on all three techniques. Differences proved to be not statistically different. The shaded area reflects generally accepted normal values for the Q_P/Q_S ratio of 0.95 to 1.05. 5pt PCVIPR = 5-point velocity-encoded radially undersampled 4D Flow MRI.

Table 1

	Total n=18	Software corrected n=11	Phantom Corrected n=11
CINE bSSFP volumetry			
LVSV	96.5 ± 14.4	97.3 ± 15.0	
RVSV	93.6 ± 14.0 *	94.3 ± 15.0 *	
2D-PC-MRI			
AAO	98.0 ± 21.8‡	99.7 ± 22.5‡	100.6 ± 27.8‡
MPA	90.0 ± 18.8 *‡	92.4 ± 17.9 *‡	95.1 ± 22.8 *‡
5-point PC-VIPR			
AAO	***81.2 ± 24.3***†	***79.6 ± 26.4*** †	95.9 ± 19.1 ‡
MPA	***85.6 ± 25.4*** *†	80.3 ± 28.8 *‡	90.3 ± 13.7 *‡
Bland-Altman (bias ± 2SD)			
LVSV vs. AAO 2D-PC-MRI	1.4 ± 22.4	2.5 ± 23.9	3.3 ± 32.1
RVSV vs. MPA 2D-PC-MRI	−3.6 ± 18.8	−1.9 ± 17.2	0.8 ± 22.1
AAO 5-point PC-VIPR vs. LVSV	−14.6 ± 44.0	−17.7 ± 48.6	−1.4 ± 15.3
MPA 5-point PC-VIPR vs. RVSV	−9.0 ± 45.9	−14.1 ± 51.7	−4.1 ± 16.1
AAO 5-point PC-VIPR vs. 2D-PC-MRI	−16.4 ± 36.2	−20.1 ± 38.4	−12.0 ±48.1
MPA 5-point PC-VIPR vs. 2D-PC-MRI	−5.5 ± 46.1	−12.2 ± 45.6	−2.2 ± 19.5
Correlation R^2			
LVSV vs. AAO 2D-PC-MRI	0.79	0.76	0.66
RVSV vs. MPA 2D-PC-MRI	0.77	0.77	0.72
AAO 5-point PC-VIPR vs. LVSV	0.23	0.18	0.86
MPA 5-point PC-VIPR vs. RVSV	0.21	0.20	0.71
AAO 5-point PC-VIPR vs. 2D-PC-MRI	0.51	0.39	0.89
MPA 5-point PC-VIPR vs. 2D-PC-MRI	0.25	0.83	0.80

‡ p = n.s. vs. contralateral;

‡ p = n.s. vs. CINE-bSSFP;

† ***p < 0.05 vs. CINE-bSSFP***